Characterizing the influence of matrix ductility on damage phenomenology in continuous fiber-reinforced thermoplastic laminates undergoing quasi-static indentation

A. Yudhanto, H. Wafai, G. Lubineau, R. Yaldiz, N. Verghese

PII: S0263-8223(17)33628-0
DOI: https://doi.org/10.1016/j.compstruct.2017.12.028
Reference: COST 9185

To appear in: *Composite Structures*

Please cite this article as: Yudhanto, A., Wafai, H., Lubineau, G., Yaldiz, R., Verghese, N., Characterizing the influence of matrix ductility on damage phenomenology in continuous fiber-reinforced thermoplastic laminates undergoing quasi-static indentation, *Composite Structures* (2017), doi: https://doi.org/10.1016/j.compstruct.2017.12.028

Characterizing the influence of matrix ductility on damage phenomenology in continuous fiber-reinforced thermoplastic laminates undergoing quasi-static indentation

A. Yudhanto*[,a], H. Wafai[a], G. Lubineau*[,a], R. Yaldiz[b], N. Verghese[b]

[a] *King Abdullah University of Science and Technology (KAUST), Physical Science and Engineering Division, COHMAS Laboratory, Thuwal 23955-6900, Saudi Arabia*
[b] *SABIC Specialties, T&I Composites, P.O. Box 319, 6160 AH Geleen, The Netherlands*

Abstract

The use of thermoplastic matrix was known to improve the impact properties of laminated composites. However, different ductility levels can exist in a single family of thermoplastic matrix, and this may consequently modify the damage phenomenology of thermoplastic composites. This paper focuses on the effect of matrix ductility on the out-of-plane properties of thermoplastic composites, which was studied through quasi-static indentation (QSI) test that may represent impact problem albeit the speed difference. We evaluated continuous glass-fiber reinforced polypropylene thermoplastic composites (GFPP), and selected homopolymer PP and copolymer PP that represent ductile and less ductile matrices, respectively. Several cross-ply laminates were selected to study the influence of ply thicknesses and relative orientation of interfaces on QSI properties of GFPP. It is expected that GFPP with ductile matrix improves energy absorption of GFPP. However, the damage mechanism is completely different between GFPP with ductile and GFPP with less ductile matrices. GFPP with ductile matrix exhibits smaller damage zone in comparison to the one with less ductile matrix. Higher matrix ductility inhibits the growth of ply cracking along the fiber, and this causes the limited size of delamination. The stacking sequence poses more influence on less ductile composites rather than the ductile one.

Keywords: A. Polymer-matrix composites (PMCs), A. Thermoplastic resin, B. Delamination, D. Mechanical testing

1. Introduction

The use of thermoplastic composites in mass-production industry, e.g., automotive, has been steadily growing over a decade. Thermoplastic composites offer various advantages: short manufacturing time, recyclable, unlimited shelf-life, and excellent impact properties [1]. Regarding impact properties, the impact damage in thermoplastic composite, such as carbon/PEEK and carbon/PPS, was found to be smaller than that in thermoset composites (carbon/epoxy) [2]. Such damage isolation capability in thermoplastic composite subsequently changed its compression-after-impact failure mechanism [3].

Impact testing poses several challenges, such as high equipment cost and limited data (namely, energy absorption, impact damage after testing, maximum force during impact). The stage-by-stage evolution of damage mechanisms on a composite during impact, which consists of the competition between various damage modes (transverse crack, delamination, fiber breakage), is difficult to track in detail. Nonetheless, Choi et al. [4] reported an experimental investigation of a damage sequence in cross-ply laminates that consists of initiation of matrix crack at the distal face, transition from transverse crack to delamination, development of an array of micro-cracks, and complete failure. However, the investigation was performed on simple beam-type laminates. Monitoring damage mechanisms during impact in plate-type laminates may require advanced instruments such as a high-speed camera [5].

One cost-effective approach used to understand the damage mechanisms under other out-of-plane loadings is quasi-static indentation (QSI) [6]. A QSI test is performed by indenting a plate with a metal rod (indenter) until a certain force or displacement is achieved. The speed of QSI is rather low (according to the ASTM standard, the loading speed is 1.25 mm/min). Although QSI is slower than a low-velocity impact (LVI), the damage modes in composite laminates under QSI load resemble those under LVI load [7, 8, 9]. The study of QSI and LVI properties of composite has been mostly reported for thermoset composites [10, 11, 12, 13, 8, 7, 14, 15, 16, 17, 18] where various factors were considered, such as ply

Email addresses: arief.yudhanto@kaust.edu.sa (A. Yudhanto*), gilles.lubineau@kaust.edu.sa (G. Lubineau*)

thickness [14], stacking sequence [19], and matrix materials [19, 7]. Very few studies on QSI or LVI properties were reported on thermoplastic composites, for instance, glass-reinforced polypropylene (GFPP). Impact performance of GFPP, specifically under repeated impact loads, was found to be better than thermoset-based composites, e.g., glass-reinforced epoxy [20]. PP is one of the most popular thermoplastic matrices used for making thermoplastic-based composites. PP is abundant and cheap to produce. As a semi-crystalline polymer, PP consists of both crystalline and amorphous phases, where the amorphous phase contains isotactic and atactic PP. Homopolymer is the basic building block of PP, containing only PP monomer, of which there are many varieties. One variant, called copolymer PP, is created by adding certain amount of rubber to improve impact (and other high-strain rate) properties of PP and PP-based composites. Since PP may come in various types, it is important to study the QSI properties of GFPP with different PP matrices to support the material selection process. Studies on the effect of matrix on out-of-plane properties (impact) have actually been reported on thermoset-type composites [21], and they suggested that (i) higher resin volume fraction ranging between 40 to 45 % could lead to a smaller impact damage since plastic deformation is facilitated, (ii) a more ductile matrix reduces impact damage size in carbon/epoxy.

Here, our objective is to study the effect of ductile and less ductile matrices of the same polypropylene family on the QSI properties and damage phenomenology of continuous GFPP thermoplastic composites. The ductile matrix is represented by the homopolymer PP, and a less ductile matrix is represented by the copolymer PP, which is homopolymer PP with ethylene-propylene rubber particles and a maleic anhydride nucleating agent added to it. We also study the influence of stacking sequence on the damage phenomenology by selecting three cross-ply laminates that could activate different damage mechanisms, namely $(90_2/0_2)_s$, $(90/0)_{2s}$ and $(90_2/\pm45)_s$. Because $(90_2/0_2)_s$ has evidently a thicker (90) outer ply than $(90/0)_{2s}$, the transition from transverse crack to delamination should proceed differently during out-of-plane loading. $(90_2/\pm45)_s$ is a modification of $(90_2/0_2)_s$ with $(\pm45)_s$ inner plies instead of $(0)_4$, and the angle-difference between (90) and (±45) plies would change the damage mechanism. We favored cross-ply configuration over quasi-isotropic due to its

relevance to the automotive industry. In the over-molding process of an automotive structure (e.g., car bumper), cross-ply can be adopted as a simple, outer protective layer for the beam component. Additionally, in the development of laminated composite model under out-of-plane load, it is generally preferred to have cross-ply laminate as a benchmarking case for theoretical or numerical prediction [11, 22, 23, 13, 24].

We firstly performed monotonic QSI test to obtain maximum load (F_{max}), maximum displacement (s_{max} or a corresponding displacement at F_{max}), total energy (E_T) at s_{max} and at limit displacement (s_{lim} = 21 mm, i.e. indenter has fully penetrated the plate), and the stage-by-stage damage process, which was captured in real-time using a digital camera with backlighting, taking an advantage of GFPP's translucence. We also performed a load/unload QSI test to measure the energy absorption (E_a) and the projected damage area at various displacement levels. Internal damage in the specimens from the load/unload QSI test was studied by dissecting the indented area and inspecting its cross-section under a scanning electron microscope (SEM). Acknowledging that impact degradations in the form of delamination and fiber breakage typically occur in the subsurface of composites and are often not visible, we also measured the permanent deformation in specimens after the load/unload QSI test by probing the depth of the indented region (dent-depth). Dent depth has been used to determine damage level [25], threshold of barely-visible impact damage (BVID) [14], and to develop its relationship with residual strength [22]. In our case, we used the correlation between dent-depth and energy absorption in order to differentiate the QSI response of GFPP laminates made from ductile (homopolymer PP) and less ductile (copolymer PP) matrices.

2. Experiments

2.1. Materials and manufacture of laminates

We used continuous E-glass fiber polypropylene (GFPP) thermoplastic composite, that was provided in the form of unidirectional (UD) tape (width = 110 mm, thickness = 0.25 mm). Two types of PP, homopolymer and copolymer, were employed to produce GFPP

tape. Melt flow rate (at 230°C and 2.16 kg) of homopolymer and copolymer was 120 dg/min and 100 dg/min, respectively. The density of both matrices was 910 kg/m^3 for homopolymer and 905 kg/m^3 for copolymer. GFPP laminates ($(90_2/0_2)_s$, $(90/0)_{2s}$, and $(90_2/\pm45)_s$) were manufactured using a static press method (Pinette Emidecau Industries 15 Tons, PEI 15T) and metallic molds (either aluminum or steel mold depending on the material). GFPP homopolymer laminate was processed by inserting the tapes (size of prepared tape was 250 mm × 110 mm) into the aluminum mold, which might produce homopolymer plate with fewer crystals (dendrites) than the steel mold. GFPP copolymer was inserted into the steel mold, and 275 mm × 110 mm plate was obtained. The typical thickness of the resulting plates was 2 mm. The plates were then cut into a rectangular specimen of 110 mm × 110 mm. A schematic of the cycle description (pressure and temperature) and the molds are shown in Fig. 1. These processing conditions and their effects on GFPP plates, particularly internal process-induced strains, have been thoroughly investigated using fiber Bragg gratings (FBGs) by the authors [26].

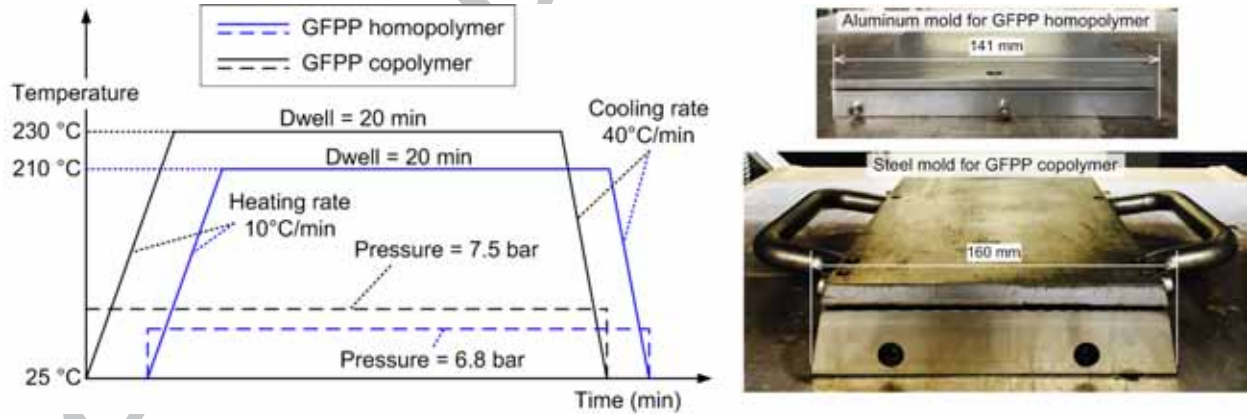

Figure 1: Schematic of cycle description and metallic molds for processing GFPP homopolymer and GFPP copolymer laminates using static hot press.

After manufacturing process, the fiber distribution was studied by using an optical microscope (Leica DM2500 M) on polished cross-sections of GFPP laminates. Fig. 2 shows that the fiber distribution in both laminates is a layered fiber cluster with resin-rich region between the clusters. We also measured the fiber volume fraction (V_f) of the GFPP tapes

and cross-ply laminates by conducting a burn-off test (ASTM D2584-11), and provide the values in Table 1. V_f of GFPP homopolymer is 44.1-45.2%, while that of GFPP copolymer is 38.7-41.6%. V_f measured on the tape is higher than that on the laminate. Sampling location on the tape may affect the measurement. The UD tape samples taken from the middle region of the tape typically have a higher fiber content than those taken from the edges.

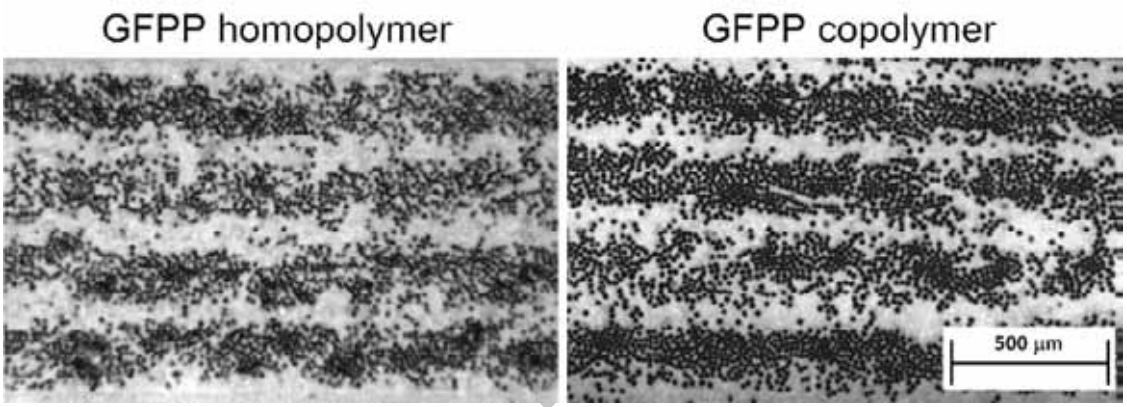

Figure 2: Fiber arrangement in GFPP homopolymer and GFPP copolymer.

Table 1: Fiber volume fraction of GFPP measured by burn-off test.

Sample type	Homopolymer	Copolymer
Unidirectional tape	45.2 ± 6.9 %	41.6 ± 2.6 %
Laminate	44.1 ± 1.3 %	38.7 ± 1.9 %

2.2. Mechanical test procedures

Tensile strength, Young's modulus and failure strain of neat polypropylene (both homopolymer and copolymer) and glass/polypropylene composites were obtained by conducting monotonic tensile test at 0.001/s strain rate. We used Instron 5944 (2 kN load cell) for obtaining tensile properties of neat PP, as well as GFPP $(90)_8$ and $(\pm 45)_s$. PP samples complied with the ISO 527-1BA standard (dumb-bell shaped with the dimensions of 75 mm long, 5 mm wide, 2 mm thick, and a gauge length of 50 mm). The sample dimension for

GFPP $(90)_8$ was 110 mm long, 20 mm wide, and 2 mm thick. The sample dimension for GFPP $(\pm 45)_s$ was 110 mm long, 9 mm wide, and 1 mm thick. The strains were measured using digital image correlation (DIC) technique. We also used Instron 5882 (100 kN load cell) to measure GFPP $(0)_4$ tensile properties. The specimen dimension of GFPP $(0)_4$ was 250 mm long, 150 mm gauge length, 15 mm wide and 1 mm thick (ASTM D-3039 Standard). The strains were measured using video extensometer.

The quasi-static indentation (QSI) test was performed using an in-house fixture fitted in the Instron 5882 (100 kN load cell) (see Fig. 3a). Test matrix for QSI is shown in Table 2. We used 16 samples (4 specimens for monotonic QSI, 12 specimens for load/unload QSI) of each specimen type. After clamping the specimen by a torque of 5 kg.m (for each screw), the indentation load was applied on the specimen at 1.25 mm/min loading speed, following ASTM D6264 Standard. The indented face and the perforation at the distal face can be seen in Figs. 3b and 3c, respectively. For monotonic QSI, the specimen was loaded until it was fully perforated (up to 21 mm). Maximum force (F_{max}), maximum displacement (s_{max}), and total energy (E_T) were obtained. E_T was calculated by integrating the area under the load-displacement curve up to s_{max}:

$$E_T = \int_0^{s_{max}} F(s)\, ds \tag{1}$$

We can also calculate E_T after full penetration by replacing s_{max} with s_{lim} of 21 mm.

The load/unload QSI test was performed on the GFPP samples at displacement levels (s) of 2, 3, 4, 5, 6, and 7 mm. Two specimens were tested for each level. The force-displacement data after load/unload test was processed to calculate the energy absorption (E_a) as follows:

$$E_a = E_l - E_u \tag{2}$$

where E_l is E_T during loading phase and E_u is E_T during the unloading phase.

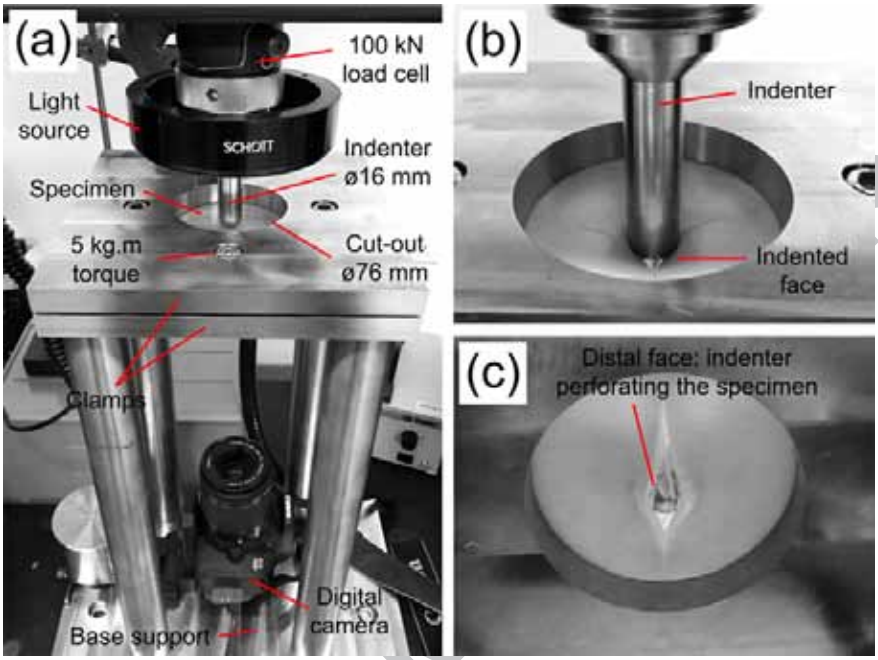

Figure 3: (a) Setup of the quasi-static indentation test; (b) penetration of the indented face; (c) perforation of the distal face.

Table 2: Test matrix for quasi-static indentation

Lay-up	PP type	Specimen quantity	
		Monotonic QSI	Load/unload QSI
$(90_2/0_2)_s$	Homopolymer	4	12
	Copolymer	4	12
$(90/0)_{2s}$	Homopolymer	4	12
	Copolymer	4	12
$(90_2/\pm 45)_s$	Homopolymer	4	12
	Copolymer	4	12

2.3. Damage observation techniques

We mainly used two techniques to observe the damage phenomenology, namely backlight method for characterizing global damage zone and scanning electron microscopy for characterizing internal damage.

A simple setup called "backlight method" was developed to capture the damage experienced by the GFPP specimens during and after QSI test. The QSI setup equipped with a circular light source is shown in Fig. 3a. The light source was Direct Current Regulated Light Source (DCR III from Schott-Fostec; 4" Maxi Ringlights from Moritex). We inserted a digital single-lens reflex (DSLR) camera (Canon 700D) underneath the QSI fixture to capture the image. The real-time images captured during QSI test enabled the reconstruction of video of damage process (however, the shadow of indenter was inevitably seen as a darker region). As such, we also took the images by removing the indenter from the specimen. The projected area of damage was subsequently measured using *ImageJ* software [27]. To validate the "backlight method", we employed an ultrasonic testing system (UltraPAC Immersion System UPK-T48-HS, Mistras Group Inc.). The specimen was immersed in water while a probe (10 MHz transducer, 2.0" focal length, 0.25" diameter) emitted pulse-echo sound wave on the specimen. UTwin for UltraPac software was used to define the parameters (time of flight and amplitude of gates), and to obtain C-scan images.

We used Quanta 600 (FEI) to perform scanning electron microscopy (SEM) in order to study the internal damage in the cross-sections of GFPP, specifically at the indented region. After load/unload QSI test, we carefully cut the specimen to prevent additional damage to the specimen. To observe initial transverse crack, we cut the specimen (after being indented at $s = 2$ mm) in the transverse direction. To observe delamination and ply fracture, we cut the specimens (after being indented at $s = 4$ and 6 mm) in the longitudinal direction. Prior to SEM process, the sample was sputtered using gold/platinum (Au/Pt) with a layer thickness of 4 nm using Emitech K575X (Quorum Technologies).

2.4. Surface profilometry

We assessed the level of plastic deformation in the GFPP plates based on a permanent dent-depth that actually reflects both the plastic deformation and the internal damage. We used a profilometer (Veeco Dektak 150) to measure the depth of the indentation. The Dektak 150 stylus probed points along a 20 mm lateral line (x-direction), and recorded the z-direction (vertical) points. The deepest point in the z-direction measurement is the dent-depth. To illustrate the dent-depth measurement procedure, consider a GFPP copolymer specimen that has been indented with $s = 4$ mm as shown in Fig. 4a. A small dent in the center of the specimen is clearly seen in Fig. 4b, where the lateral line crosses over the dent.

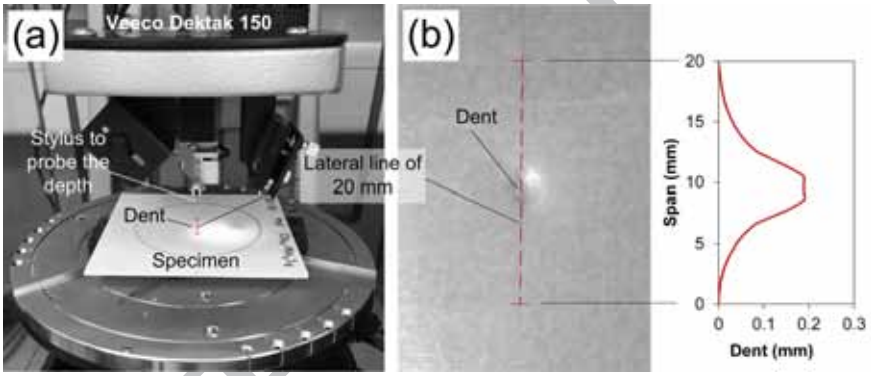

Figure 4: (a) Profilometer and specimen for dent-depth measurement; (b) position of 20-mm lateral line across the dent.

3. Results and Discussion

3.1. Tensile properties of PP and GFPP

Tensile tests were performed to determine the ductility level of PP, and its implication on the tensile properties of GFPP of basic lay-ups. The stress-strain curves and tensile properties (tensile strength, failure strain, Young's modulus) are given in Fig. 5 and Table 3, respectively. Fig. 5a and Table 3 show that the ductility of homopolymer PP is double that of copolymer PP (failure strain of copolymer is merely 2.69%). Homopolymer PP is also 68% stronger and 17% stiffer than PP copolymer. The higher ductility, strength and stiffness of PP homopolymer were evidently reflected more on matrix-dominated lay-ups rather than

the fiber-dominated one. In fiber-dominated lay-up of $(0)_4$, tensile strength and Young's modulus of GFPP homopolymer $(0)_4$ (Fig. 5b) are 13.7% and 5.3% higher, respectively, than those of GFPP copolymer. In this case, the effect of V_f (referring to Table 1, V_f of GFPP homopolymer is 14% higher than that of GFPP copolymer) is dominant since other factors (fiber longitudinal strength, and fiber clustering shown in Fig. 2) are kept similar between them. In matrix-dominated lay-ups of (90°) and (±45°), Figs. 5c-d show that the transverse strength and in-plane shear strength of GFPP homopolymer are higher than those of GFPP copolymer. However, it should be noted that the higher ductility of PP homopolymer does not reflect on the transverse failure strain shown in Fig. 5c since the transverse failure is strongly controlled by the inter-fiber distance [28].

Table 3: Tensile properties of PP and GFPP composites.

Properties	Unit	Homopolymer	Copolymer
Polypropylene			
Tensile strength	MPa	35.2 ± 0.6	21.0 ± 0.1
Failure strain	%	5.49 ± 0.46	2.69 ± 0.13
Young's modulus	GPa	2.05 ± 0.04	1.75 ± 0.16
Glass/polypropylene			
Longitudinal strength	MPa	846 ± 87	744 ± 73
Longitudinal failure strain	%	2.53 ± 0.16	2.32 ± 0.13
Longitudinal modulus	GPa	36.1 ± 1.1	34.3 ± 1.6
Transverse strength	MPa	25.3 ± 1.2	16.8 ± 0.6
Transverse failure strain	%	0.59 ± 0.11	0.50 ± 0.05
Transverse modulus	GPa	5.59 ± 0.28	4.43 ± 0.19
Shear strength	MPa	55.8 ± 2.7	32.6 ± 2.1
Shear failure strain	%	50.8 ± 3.8	32.8 ± 1.8
Shear modulus	GPa	1.35 ± 0.06	0.99 ± 0.04

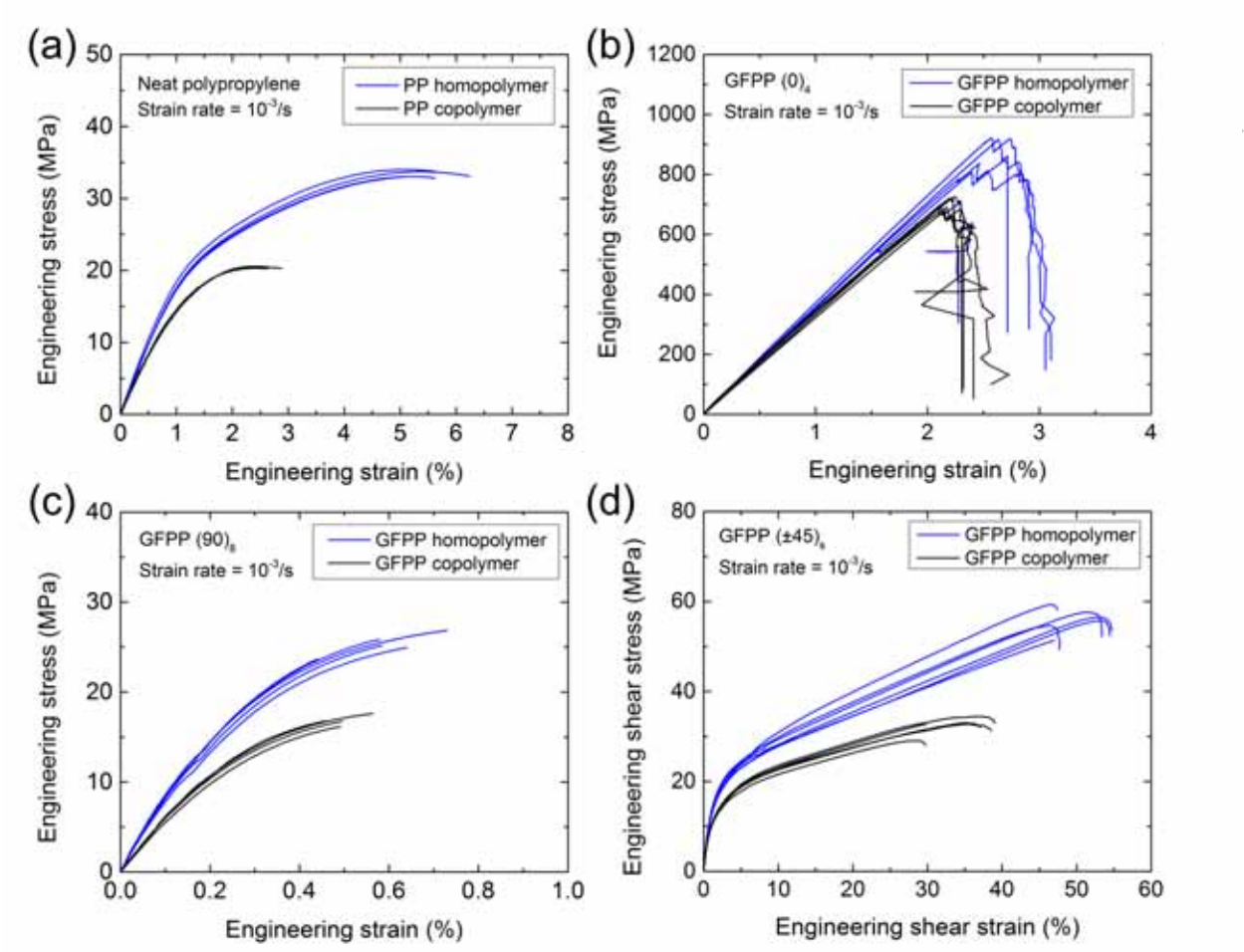

Figure 5: Tensile test results of (a) neat PP, (b) GFPP $(0)_4$ (longitudinal tensile properties), (c) GFPP $(90)_8$ (transverse tensile properties), (d) GFPP $(\pm 45)_s$ (in-plane shear properties). PP copolymer data has also been published by the authors elsewhere [29]

3.2. QSI properties of GFPP

Figs. 6a-c show the comparison of force-displacement curves between GFPP homopolymer and GFPP copolymer obtained from monotonic QSI tests. Table 4 gives the summary of the QSI properties of GFPP. GFPP with homopolymer PP generally exhibits higher F_{max} (peak force required to fracture all plies at the vicinity beneath the indenter's tip) than GFPP with copolymer PP, but this is partly driven by higher fiber volume fraction (hence, higher bending stiffness) of the GFPP homopolymer. Stacking sequence also has some influence on QSI properties. GFPP copolymer works better with $(90_2/0_2)_s$ lay-up

rather than $(90/0)_{2s}$. On the other hand, GFPP homopolymer works better with $(90/0)_{2s}$ than $(90_2/0_2)_s$. GFPP copolymer seems to behave more like a thermoset laminate [14], i.e. downscaling the ply thickness (hence, thin plies) improves the load-bearing capability due to the energy dissipation through multiple delaminations (as later shown by SEM investigation). On the contrary, downscaling the ply thickness in GFPP homopolymer reduces the maximum force since the energy dissipation was mostly made through an immediate, local laminate fracture.

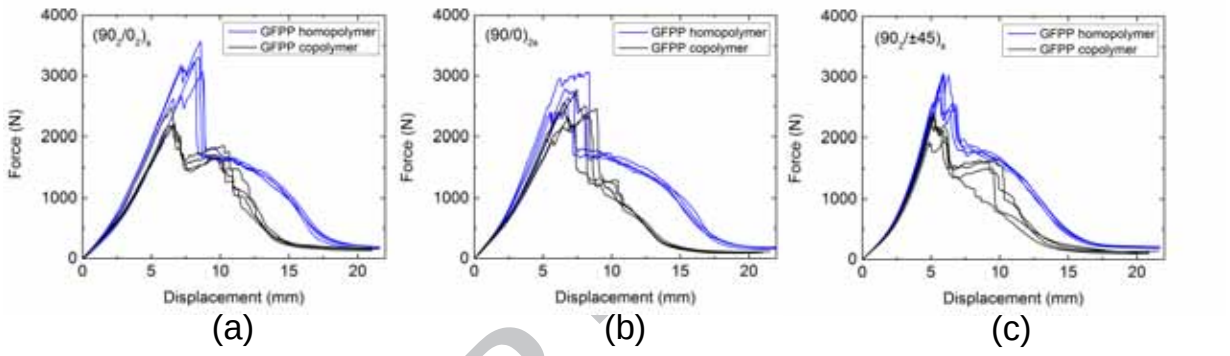

Figure 6: Force-displacement curves from monotonic QSI test of (a) $(90_2/0_2)_s$, (b) $(90/0)_{2s}$, (c) $(90_2/\pm45)_2$.

Table 4: QSI properties of GFPP homopolymer and GFPP copolymer laminates (s_{lim} = 21 mm).

Lay-up	PP type	F_{max} (N)	s_{max} (mm)	E_T (J) at s_{max}	E_T (J) at s_{lim}
$(90_2/0_2)_s$	Homopolymer	3293 ± 209	8.48 ± 0.24	13.0 ± 0.9	25.3 ± 1.5
	Copolymer	2262 ± 147	6.59 ± 0.08	6.6 ± 0.4	17.6 ± 1.3
$(90/0)_{2s}$	Homopolymer	2765 ± 232	7.26 ± 0.75	10.0 ± 2.7	24.3 ± 1.4
	Copolymer	2505 ± 189	7.81 ± 1.00	9.9 ± 1.9	16.7 ± 0.4
$(90_2/\pm45)_s$	Homopolymer	2910 ± 180	5.78 ± 0.14	6.4 ± 0.2	21.5 ± 0.5
	Copolymer	2269 ± 216	5.36 ± 0.37	4.8 ± 0.5	15.2 ± 1.4

We used energy absorption (E_a) to evaluate GFPP homopolymer and GFPP copolymer since it may include the damage development within composites [23, 25, 30]. We calculated E_a for each specimen using load/unload data shown in Fig. 7 and Eq. 2. The relationship

between E_a and F_{max} is shown on the right-hand graphs of Fig. 7. For $(90_2/0_2)_s$ and $(90_2/\pm45)_s$, GFPP copolymer evidently absorbs more energy than GFPP homopolymer through the development of a larger damage zone (as later shown in the next section). E_a of GFPP homopolymer and GFPP copolymer with $(90/0)_{2s}$ is similar, indicating that thin plies promotes similar damage mechanism albeit ductility difference between two matrices.

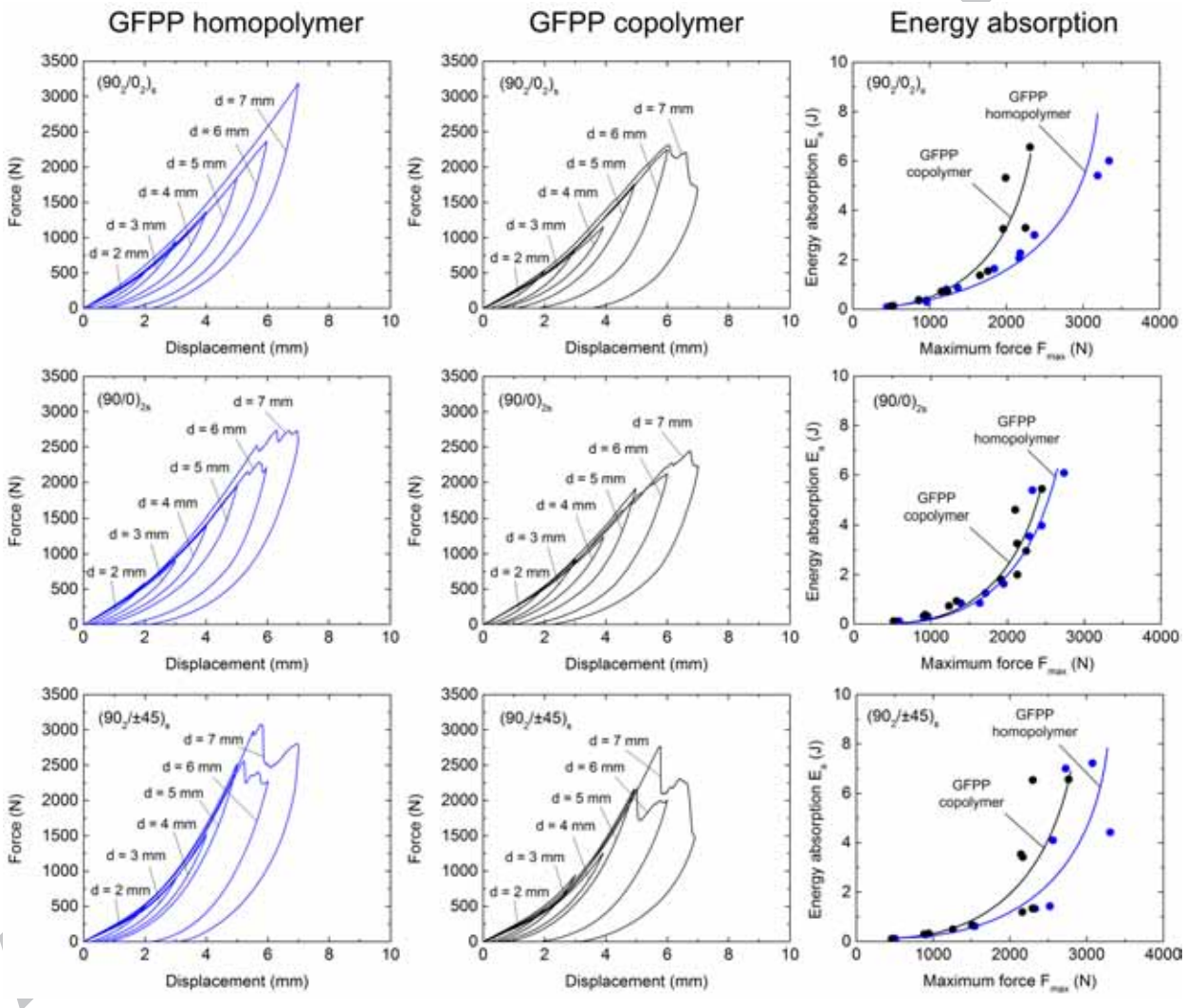

Figure 7: Load/unload QSI test results for GFPP homopolymer and GFPP comopolymer

3.3. Damage phenomenology

Fig. 8 shows the images of GFPP homopolymer and GFPP copolymer subjected to different displacement levels (s = 2 mm, 4 mm, 6 mm) obtained from backlight method

(with removal of the indenter), where the darker regions represent the damage zone. We compared one of the backlight images with the result from ultrasonic C-scan, and as shown in Fig. 9, the damage zone obtained by backlight method and C-scan is quite similar, indicating that the backlight method is justified in capturing the global damage zone in GFPP.

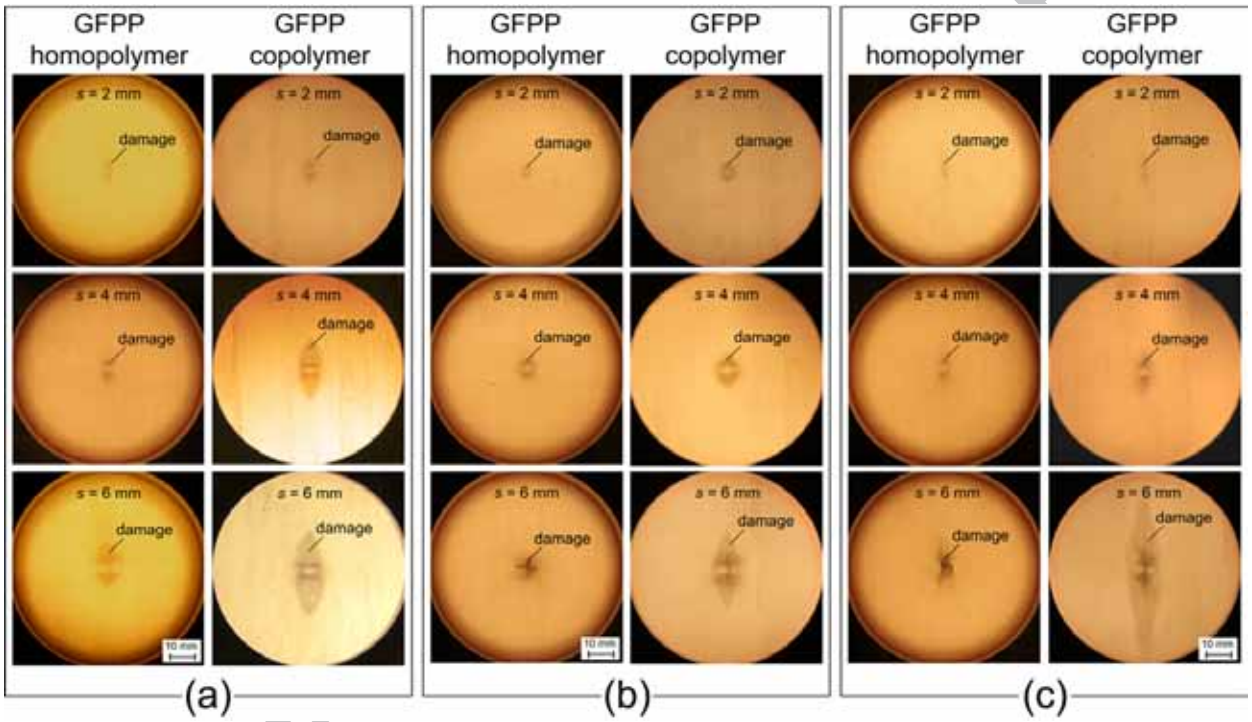

Figure 8: Damage evolution in GFPP homopolymer and GFPP copolymer: (a) $(90_2/0_2)_s$, (b) $(90/0)_{2s}$, (c) $(90_2/\pm 45)_s$. Note: Readers could also download some videos reconstructed based on the backlight images for $(90_2/0_2)_s$ laminates in video format files. Here, we demonstrated that the backlight method is effective in capturing the progression of damage in GFPP in real-time.

Backlight images in Fig. 8 have already shown that at $s = 2$ mm damage in GFPP has been initiated. After cutting the specimens perpendicular to (90°) ply, we found that the earliest damage mode was transverse crack, which was initiated from the distal face of (90°) ply (see SEM images in Fig. 10). The damage mode is the same for both GFPP homopolymer and GFPP copolymer, and this confirms that the earliest damage mode, i.e. transverse crack, was independent of matrix ductility. As mentioned, the transverse crack

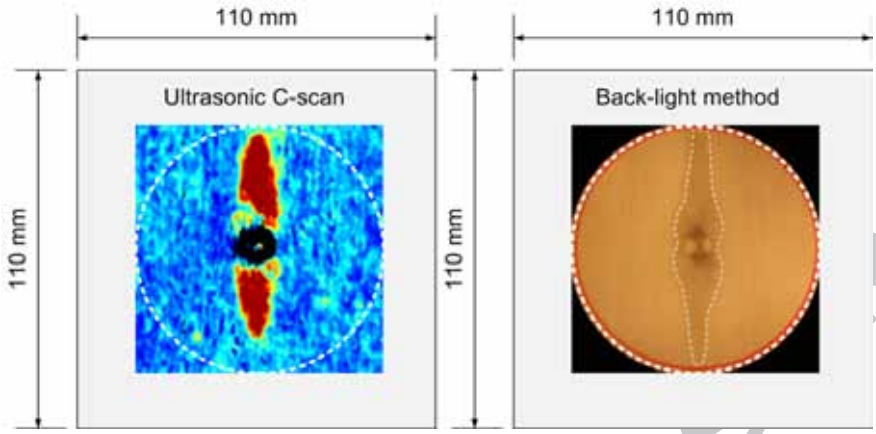

Figure 9: Comparison between ultrasonic C-scan and backlight method for GFPP copolymer of $(90_2/\pm 45)_s$ lay-up.

is guided by the inter-fiber distance [28].

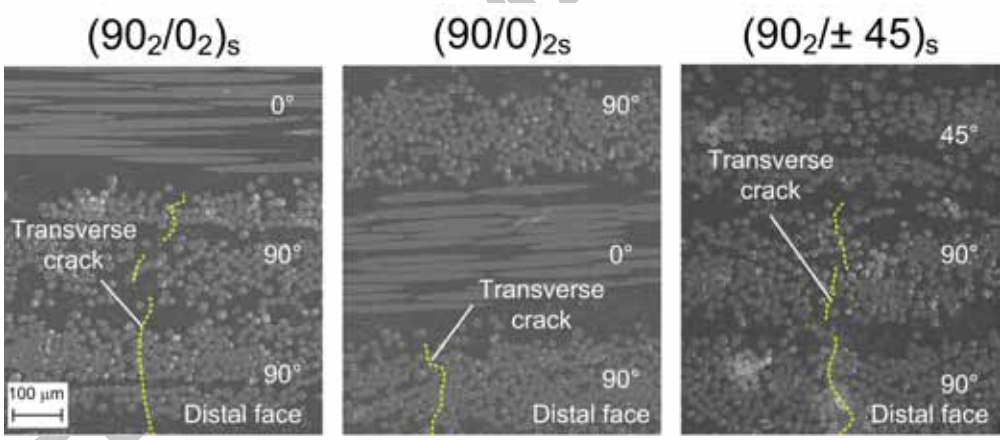

Figure 10: Scanning electron microscopy results on the cross-section area of specimens cut perpendicular to (90°) ply of indented region after being subjected to QSI load/unload at $s = 2$ mm.

Damage progression in GFPP, on the other hand, is affected by the type of PP matrix. Fig. 8 shows that the damage zone for all studied lay-ups in GFPP copolymer is generally more extensive than that in GFPP homopolymer. SEM images displayed in Fig. 11 also confirm that although the same damage types (transverse crack, delamination, local dent or surface damage, ply fracture) exist in both GFPP homopolymer and GFPP copolymer, but the size of delamination was different. GFPP copolymer shows longer delamination than

GFPP homopolymer. The corresponding mechanisms for each PP type can be summarized as follows:

- The localized damage in GFPP homopolymer (the ductile matrix) is characterized by the limited extent of delamination, local dent due to the indenter, ply fracture and multiple localized delaminations. The localized damage in GFPP homopolymer is strongly related to a short transverse crack that was developed along (90°) ply in the distal face. This is mostly governed by high Mode I fracture toughness in GFPP homopolymer [31]. As a result, the indentation energy in GFPP homopolymer was subsequently dissipated through: (i) the bending of the intact plies and permanent deformation at the indented face, (ii) the transition from transverse crack into delamination.

- The extensive damage in GFPP copolymer (the less ductile matrix) is characterized by relatively large delamination, multiple delaminations at several interfaces as well as ply fracture. The extensive damage was caused by the fact that the transverse crack easily propagated along (90°) ply due to low Mode I fracture toughness, inducing relatively large delamination in the distal (0/90) interface. Larger delamination in GFPP copolymer is plausibly caused by its lower Mode II fracture toughness in comparison to GFPP homopolymer [31, 32].

The effect of stacking sequence on the damage progression in GFPP copolymer and GFPP homopolymer is briefly discussed herein. In GFPP copolymer, both $(90_2/0_2)_s$ and $(90_2/\pm45)_s$ exhibit a larger damage zone than $(90/0)_{2s}$, meaning that the thinner plies in GFPP copolymer is effective in reducing the damage zone. In GFPP homopolymer, the stacking sequence did not affect much the size of damage zone, except in the case of $(90_2/0_2)_s$. Here, thicker plies and large angle difference at the interface (between (90°) and (0°)) caused relatively larger damage zone in comparison to $(90/0)_{2s}$ and $(90_2/\pm45)_s$, respectively.

At final stage ($s = 21$ mm), we obtained the photographs and backlight images of the specimens, and they are shown in Figs. 12a-c. At the indented face, the photographs show that all specimens generated similar local dent. Backlight images show that GFPP

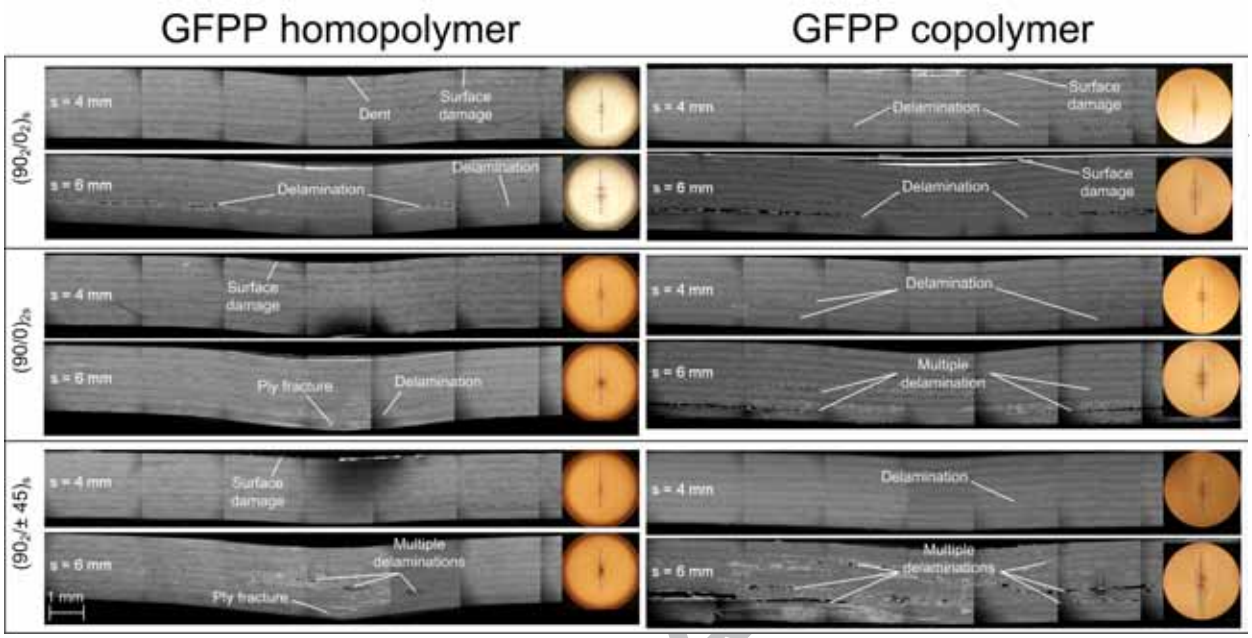

Figure 11: Scanning electron microscopy results on the cross-section area of specimens cut along (90°) ply of indented region after being subjected to QSI load/unload at $s = 4$ mm and 6 mm.

homopolymer consistently exhibited localized damage, but at this point four "petals" were clearly formed. GFPP copolymer exhibited local puncture of plies with an extensive delamination and ply splitting at the distal face, reaching the plate boundary.

Summary of damage mechanism is given in Fig. 13. In GFPP homopolymer with thick and thin plies, transverse crack growing in longitudinal direction is rather limited. As such, delamination is also small. In contrast, the growth of transverse crack in GFPP copolymer is quite extensive, and delamination is consequently larger than that in GFPP homopolymer.

3.4. Energy dissipation mechanism

Figs. 14a-c show the relationship between the energy absorption and the permanent deformation (which is represented by the dent-depth). Both GFPP homopolymer and GFPP copolymer exhibit similar level of permanent plastic deformation for all studied lay-ups. Since dent depth represents a very local deformation, it may not be a proper indicator to differentiate the effect of matrix ductility on the energy absorption of GFPP under QSI. On the other hand, Figs. 15a-c show that the energy absorption is proportional to the damage

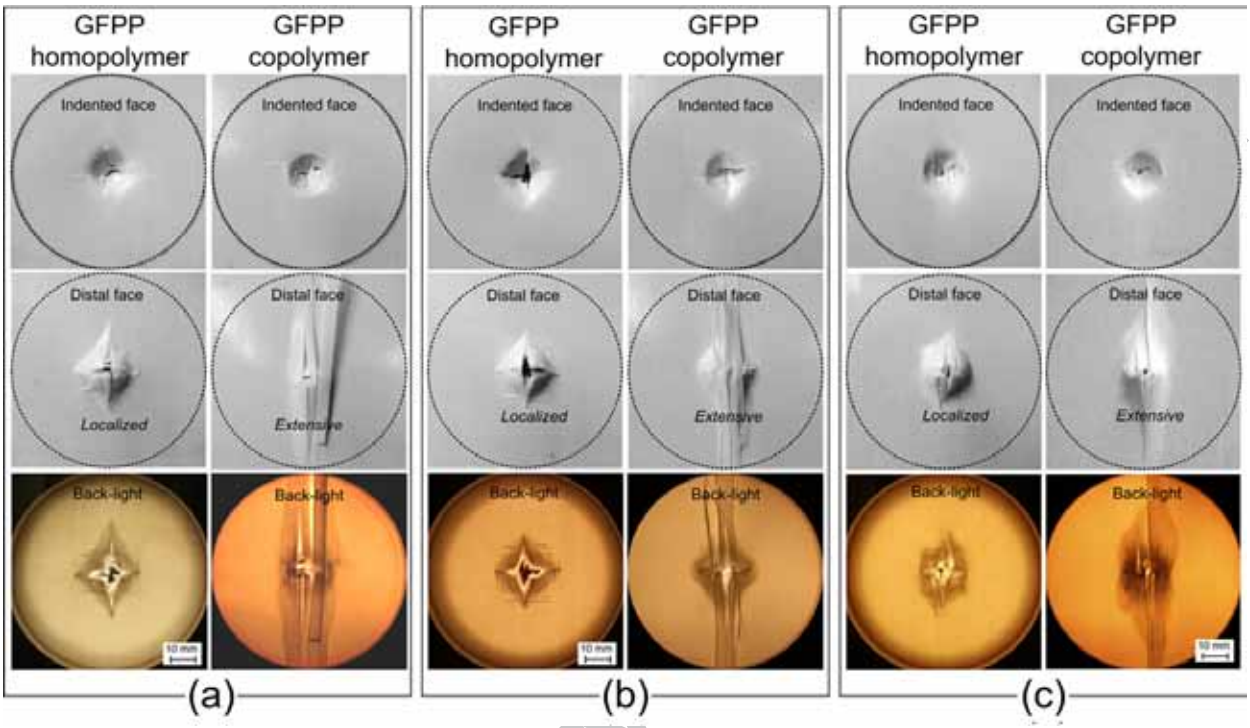

Figure 12: Failure mode of monotonic QSI test samples observed in the indented face and the distal face, and the backlight image: (a) $(90_2/0_2)_s$; (b) $(90/0)_{2s}$; (c) $(90_2/\pm 45)_s$.

area (measured based on the backlight results), indicating that damage-energy absorption relationship, which is quite linear, can be used to differentiate effect of matrix ductility on GFPP. Here, GFPP copolymer clearly absorbs more energy through damage than GFPP homopolymer. Damage-energy relationship in GFPP homopolymer is less sensitive to the stacking sequence, indicating that GFPP homopolymer is more versatile than GFPP copolymer. When GFPP copolymer is to be utilized, it is suggested to select $(90/0)_{2s}$ since damage can be well-reduced.

4. Conclusions

We studied the quasi-static indentation (QSI) response of thermoplastic composites using continuous glass-fiber polypropylene (GFPP) laminates with three different cross-ply stacking sequences and two different matrices, homopolymer PP (ductile) and copolymer PP (less ductile). Several conclusions can be made herein. Ductile matrix improves maximum force

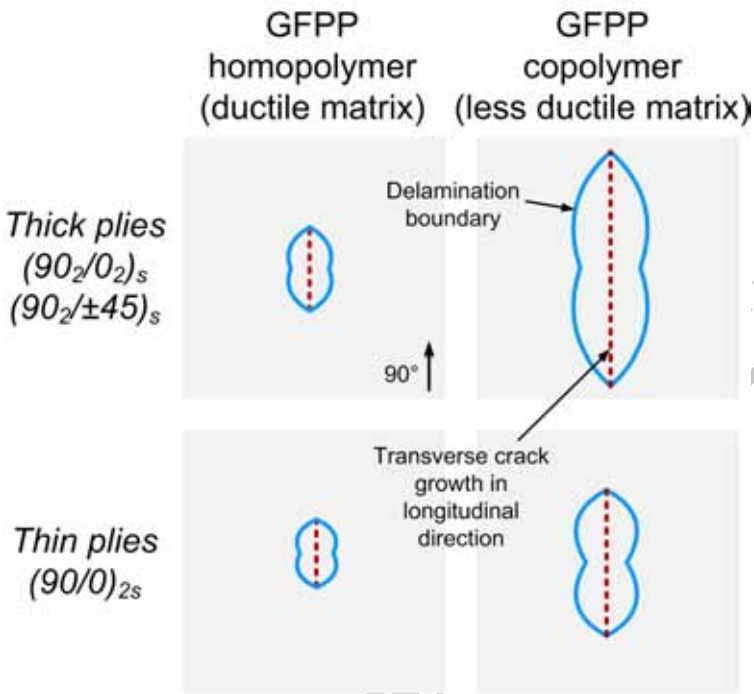

Figure 13: Summary of damage mechanism in GFPP homopolymer and copolymer.

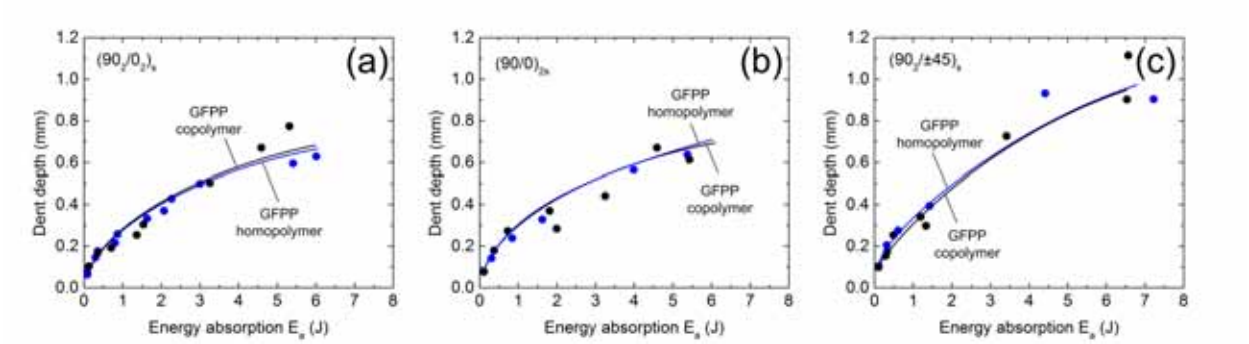

Figure 14: Relationship between energy absorption and dent-depth: (a) $(90_2/0_2)_s$, (b) $(90/0)_{2s}$, (c) $(90_2/\pm45)_s$.

and total energy of GFPP under QSI regardless of the stacking sequence. Damage initiation in GFPP is similar regardless of the matrix ductility and stacking sequence, which is transverse crack at the distal face of (90) ply. Transverse crack is mainly guided by the inter-fiber distance within the ply so changing the matrix ductility does not change the through thickness initiation stage. However, the longitudinal propagation of the transverse crack changes with the ductility of the matrix: GFPP with ductile matrix exhibits a shorter crack length

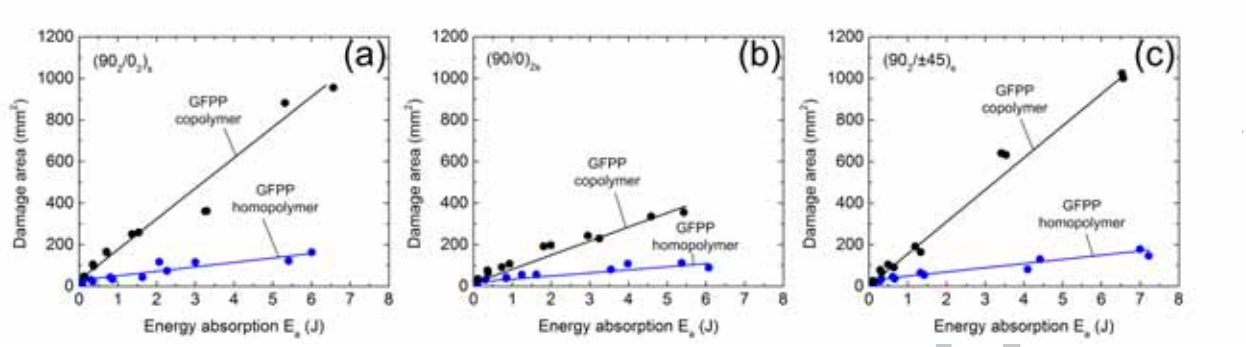

Figure 15: Relationship between energy absorption and damage area: (a) $(90_2/0_2)_s$, (b) $(90/0)_{2s}$, (c) $(90_2/\pm45)_s$.

along the fiber direction than GFPP with less ductile matrix. During progression and final stages, GFPP with ductile matrix exhibits a localized damage, while that with less ductile matrix exhibits more extensive damage as the transition from transverse cracking to delamination is facilitated. The relationship between energy absorption and damage area can be used to gauge the effect of matrix ductility in GFPP, regardless of the stacking sequence. The results of this study can be useful to support material selection stage when thermoplastic composites with simple cross-ply lay-ups are considered for designing impact-prone structures.

Acknowledgments

The research reported in this publication was supported by SABIC and by the King Abdullah University of Science and Technology (KAUST). We thank Mr. Warden Schijve (SABIC) and Mr. Ditho Pulungan (COHMAS, KAUST) for the discussion, Mr. Ran Tao (COHMAS, KAUST) for assisting with the dent-depth measurement, Dr. Lutfan Sinatra (Functional Nanomaterial Laboratory, KAUST) for assisting with the burn-off test and Mr. Shiva Goutham (COHMAS, KAUST) for assisting with the tensile tests, Mr. Guillaume Ratouit (SABIC) and Mr. Rob Marrees (SABIC) for assisting with C-scan.

References

[1] R. Stewart. Thermoplastic composites recyclable and fast to process. *Reinforced Plastics*, 55(3):22–28, 2011.

[2] B. Vieille, V. M. Casado, and C. Bouvet. About the impact behavior of woven-ply carbon fiber-reinforced thermoplastic- and thermosetting-composites: A comparative study. *Composite Structures*, 101:9–21, 2013.

[3] B. Vieille, V. M. Casado, and C. Bouvet. Influence of matrix toughness and ductility on the compression-after-impact behavior of woven-ply thermoplastic- and thermosetting- composites: A comparative study. *Composite Structures*, 110:207–218, 2014.

[4] H. Y. Choi, R. J. Downs, and F. K. Chang. A new approach toward understanding damage mechanisms and mechanics of laminated composites due to low-velocity impact: Part I Experiments. *Journal of Composite Materials*, 25:992–1011, 1991.

[5] B. Pan, Li. Yu, Y. Yang, W. Song, and L. Guo. Full-field transient 3D deformation measurement of 3D braided composite panels during ballistic impact using single-camera high-speed stereo-digital image correlation. *Composite Structures*, 157:25–32, 2016.

[6] L. S. Sutherland and C. Guedes Soares. The use of quasi-static testing to obtain the low-velocity impact damage resistance of marine GRP laminates. *Composites Part B: Engineering*, 43(3):1459–1467, 2012.

[7] D. J. Bull, S. M. Spearing, and I. Sinclair. Investigation of the response to low velocity impact and quasi-static indentation loading of particle-toughened carbon-fibre composite materials. *Composites Part A: Applied Science and Manufacturing*, 74:38–46, 2015.

[8] E. A. Abdallah, C. Bouvet, S. Rivallant, B. Broll, and J. J. Barrau. Experimental analysis of damage creation and permanent indentation on highly oriented plates. *Composites Science and Technology*, 69(7-8):1238–1245, 2009.

[9] Y. Aoki, H. Suemasu, and T. Ishikawa. Damage propagation in CFRP laminates subjected to low velocity impact and static indentation. *Advanced Composite Materials*, 16(1):45–61, 2007.

[10] S. A. Hitchen and R. M. J. Kemp. The effect of stacking sequence on impact damage in a carbon fibre/epoxy composite. *Composites*, 26(3):207–214, 1995.

[11] G. Caprino, V. Lopresto, C. Scarponi, and G. Briotti. Influence of material thickness on the response of carbon-fabric/epoxy panels to low velocity impact. *Composites Science and Technology*, 59:2279–2286, 1999.

[12] D. D. Symons. Characterisation of indentation damage in 0/90 lay-up T300/914 CFRP. *Composites Science and Technology*, 60:391–401, 2000.

[13] M. F. S. F. de Moura and J. P. M. Gonçalves. Modelling the interaction between matrix cracking and delamination in carbon-epoxy laminates under low velocity impact. *Composites Science and Technology*,

64(7-8):1021–1027, 2004.

[14] E. Abisset, F. Daghia, X.C. Sun, M.R. Wisnom, and S.R. Hallett. Interaction of inter- and intralaminar damage in scaled quasi-static indentation tests: Part 1 Experiments. *Composite Structures*, 136:712–726, feb 2016.

[15] M. L. Benzeggagh and S. Benmedakhene. Residual strength of a glass/polypropylene composite material subjected to impact. *Composites Science and Technology*, 55:1–11, 1995.

[16] O. A. Khondker, X. Yang, N. Usui, and H. Hamada. Mechanical properties of textile-inserted PP/PP knitted composites using injection compression molding. *Composites Part A: Applied Science and Manufacturing*, 37:2285–2299, 2006.

[17] B. Alcock, N. O. Cabrera, N. M. Barkoula, and T. Peijs. Low velocity impact performance of recyclable all-polypropylene composites. *Composites Science and Technology*, 66:1724–1737, 2006.

[18] P. Russo, D. Acierno, G. Simeoli, S. Iannace, and L. Sorrentino. Flexural and impact response of woven glass fiber fabric/polypropylene composites. *Composites Part B*, 54:415–421, 2013.

[19] P. Chen, Z. Shen, J. Xiong, S. Yang, S. Fu, and L. Ye. Failure mechanisms of laminated composites subjected to static indentation. *Composite Structures*, 75:489–495, 2006.

[20] V. Arikan and O. Sayman. Comparative study on repeated impact response of E-glass fiber reinforced polypropylene & epoxy matrix composites. *Composites Part B*, 83:1–6, 2015.

[21] J. G. Williams and M. D. Rhodes. Effect of resin on impact damage tolerance of graphite/epoxy laminates. *ASTM International, Composite Materials: Testing and Design (Sixth Conference)*, pages 450–480, 1982.

[22] G. Caprino and V. Lopresto. The significance of indentation in the inspection of carbon fibre-reinforced plastic panels damaged by low-velocity impact. *Composites Science and Technology*, 60(7):1003–1012, 2000.

[23] G. Caprino, A. Langella, and V. Lopresto. Elastic behaviour of circular composite plates transversely loaded at the centre. *Composites Part A: Applied Science and Manufacturing*, 33:1191–1197, 2002.

[24] E. Sitnikova, S. Li, D. Li, and X. Yi. Subtle features of delamination in cross-ply laminates due to low speed impact. *Composites Science and Technology*, 149:149–158, 2017.

[25] A. Wagih, P. Maimi, N. Blanco, and J. Costa. A quasi-static indentation test to elucidate the sequence of damage events in low velocity impacts on composite laminates. *Composites Part A: Applied Science and Manufacturing*, 82:180–189, 2016.

[26] M. Mulle, H. Wafai, A. Yudhanto, G. Lubineau, R. Yaldiz, W. Schijve, and N. Verghese. Process monitoring of glass reinforced polypropylene laminates using fiber Bragg gratings. *Composites Science and Technology*, 123:143–150, 2016.

[27] C. A. Schneider, W. S. Rasband, and K. W. Eliceiri. NIH Image to ImageJ: 25 years of image analysis.

Nature Methods, 9(7):671–675, 2012.

[28] D. Pulungan, G. Lubineau, A. Yudhanto, R. Yaldiz, and W. Schijve. Identifying design parameters controlling damage behaviors of continuous fiber-reinforced thermoplastic composites using micromechanics as a virtual testing tool. *International Journal of Solids and Structures*, 117:177–190, 2017.

[29] A. Yudhanto, G. Lubineau, H. Wafai, M. Mulle, D. Pulungan, and R. Yaldiz. Monotonic and cyclic responses of impact polypropylene and continuous glass fiber-reinforced impact polypropylene composites at different strain rates. *Polymer Testing*, 51:93–100, 2016.

[30] A. Wagih, P. Maimí, E. V. González, N. Blanco, J. R. Sainz de Aja, F. M. de la Escalera, R. Olsson, and E. Alvarez. Damage sequence in thin-ply composite laminates under out-of-plane loading. *Composites Part A: Applied Science and Manufacturing*, 87:66–77, 2016.

[31] H. Wafai, A. Yudhanto, G. Lubineau, R. Yaldiz, and N. Verghese. An in-situ micro-scale approach to forecasting the macro-scale damage behavior of thermoplastic cross-ply laminates under out-of-plane loading. *Submitted*, 2017.

[32] S. Liu. Delamination and matrix cracking of cross-ply laminates due to a spherical indenter. *Composite Structures*, 25:257–265, 1993.